Oil Shale, 2011, Vol. 28, No. 2, pp. 284–295
doi: 10.3176/oil.2011.2.03
ISSN 0208-189X

THERMOGRAVIMETRIC ANALYSIS OF THE COMBUSTION CHARACTERISTICS OF OIL SHALE SEMI-COKE/BIOMASS BLENDS

WANG QING*, XU HAO, LIU HONGPENG, JIA CHUNXIA, BAI JINGRU

Northeast Dianli University
Jilin 132012, China

The combustion behavior of different kinds of biomass (corn stalks, straw, rice husks, sawdust) and oil shale semi-coke and their blends was investigated. Non-isothermal thermogravimetric experiments were performed with different atmospheres (N_2:O_2=8:2, N_2:O_2=7:3, N_2:O_2=6:4) at a constant heating rate of 20 °C/min. The effect of oxygen concentration on the pattern of combustion was analyzed. The experimental results showed that the ignition and burnout temperatures of biomass and semi-coke decreased with increasing oxygen concentrations. Aside from the weight loss during moisture evaporation, the combustion of individual biomass and semi-coke samples took place in two stages. In the first stage, the release and combustion of volatiles took place, while in the second stage, the combustion of fixed carbon occurred. The combustion of blends took place in three stages (again aside from moisture evaporation) corresponding to the sum of the individual stages of combustion of biomass and semi-coke. Several combustion reaction kinetics mechanisms were tested using the Coats–Redfern Method in order to find the mechanisms responsible for sample combustion. The activation energy was determined assuming that single separate reactions occur in each stage of thermal conversion. The results showed that a first-order chemical reaction model provided the best characterization of the first stage of biomass oxidation and oil shale semi-coke combustion. However, diffusion was found to be responsible for the second stage of biomass and semi-coke combustion. For blends, a first-order chemical reaction provided the best model for the first and second stages of combustion whereas a diffusion mechanism was the best for the third stage.

Introduction

Oil shale semi-coke, formed in the thermal processing of oil shale, is a low-grade fuel with low volatility, low calorific value and high ash content. It is

* Corresponding author: e-mail *rlx888@126.com*

difficult to ignite and burn out. Semi-coke creates serious pollution problems to the environment. Hence, in the oil-shale industry, one of the main concerns is how to treat semi-coke effectively [1–4]. Practice has shown that the co-combustion of semi-coke and high-calorific fuels would be one of the most promising options to overcome this. Wang Q. *et al*. [5, 6] investigated the co-combustion of oil shale and its semi-coke. Their research results showed that the advance ignition could be achieved when semi-coke was mixed with raw oil shale or high-calorific fuels. Trikkel *et al.* [7] conducted a study on the combustion of semi-coke and its mixtures with small additions of oil shale in a 50 kW_{th} circulating fluidized-bed boiler (CFB) and showed that such combustion is a technically feasible method for enhancing semi-coke combustion. Arro *et al.* [8] discussed the co-combustion of oil shale and its semi-coke in a certain proportion in a CFB.

Biomass is one kind of green energy source and has many advantages, such as easy storage, high burning efficiency, low pollution, low dust and high heating value [9]. Gil *et al.* [10] proposed an appropriate coal/biomass proportion to achieve the desired combustion performance by using thermogravimetric analysis (TGA). Some researchers [11, 12] have reported the combustion of coal/biomass blends to be a more attractive way to use renewable energy.

At present, the oxygen-enriched combustion technology is gradually developing with its application range continuously expanding. Liu and Fang [13, 14] have investigated the pyrolysis and combustion of biomass in nitrogen, air and oxygen-enriched atmospheres using thermogravimetry. Yu and Luo [15, 16] found that an oxygen-enriched atmosphere could improve the combustion characteristics of biomass fuel.

So far, there has been no reported co-combustion of oil shale semi-coke and biomass at different oxygen concentrations. In this work, we focus on the investigation of the effect of oxygen concentration on the combustion performance of semi-coke/biomass blends by using a thermogravimetric analyzer. The aim is to provide a theoretical foundation for the combustion of semi-coke/biomass blends in a circulating fluidized-bed.

Experimental

Materials

The oil shale semi-coke (SC) sample used in this work was obtained from a Huadian oil-shale retort factory in Jilin Province, China. Biomass samples were also from a Huadian factory. The raw materials, including corn stalks, straw, rice husks and sawdust, were designated as CS, SW, RH, and SD, respectively. These were blended with oil shale semi-coke to prepare different binary blends with the same proportion 8:2, and were named as CSSC, SWSC, RHSC and SDSC, respectively. The ultimate and proximate analyses for the samples are presented in Table 1. All the samples were ground to a particle size of <200 μm.

Table 1. **Proximate and ultimate analyses (%) and calorific values of samples**

Sample	Proximate analysis, %				LHV, kJ/kg	Ultimate analysis, %				
	M_{ad}	V_{ad}	A_{ad}	FC_{ad}	$Q_{net,ar}$ (kJ/kg)	C_{ad}	H_{ad}	O_{ad}	N_{ad}	S_{ad}
CS	7.39	69.86	6.06	16.68	17097.38	37.95	6.47	40.76	0.77	0.59
SW	7.05	66.80	9.56	16.58	16039.85	36.55	5.49	40.01	0.78	0.56
RH	7.16	51.72	28.95	12.17	11593.73	36.31	4.05	22.9	0.51	0.12
SD	6.7	74.90	8.24	10.15	12122.71	45.55	5.42	33.31	0.60	0.17
SC	0.89	10.44	82.62	6.09	3868.29	11.29	0.35	4.21	0.11	0.53

Experimental setup and method

In this research, thermogravimetric experiments were carried out using a Perkin-Elmer (USA) thermogravimetric analyzer. The experiments were conducted using different oxygen concentrations (20%, 30% and 40%). All the experiments were carried out at a flow rate of 80 mL/min and a heating rate of 20 °C/min in the temperature range from 40 °C to ~850 °C. About 6 mg of each sample was spread in a uniform layer. All the experiments were repeated and the mean values of the resulting data were used to guarantee deviations to be within 3%.

Results and discussion

DTG curves in the air atmosphere

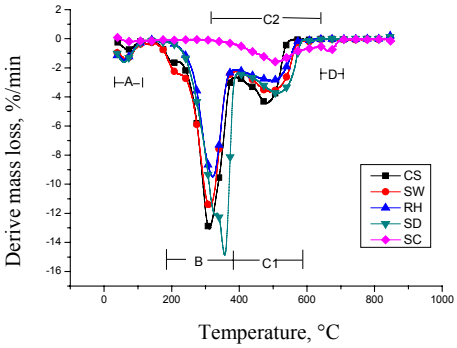

Fig. 1. DTG curves of raw biomass and oil shale semi-coke in an air atmosphere.

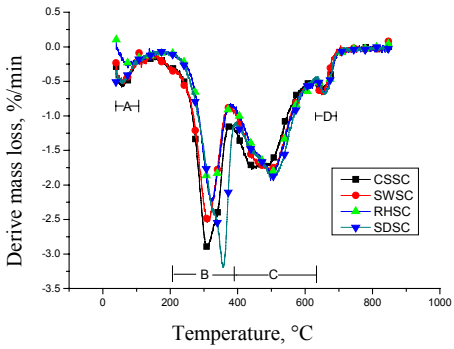

Fig. 2. DTG curves of different biomass/ oil shale semi-coke blends in an air atmosphere.

The experimental derivative thermogravimetric (DTG) curves for semi-coke and biomass and their blends in an air atmosphere are shown in Figs. 1–2. There were three stages of weight loss for the individual raw biomass and oil shale semi-coke samples, and four stages for their blends. For all samples, Stage A corresponded to moisture evaporation at temperatures ranging from 40 to 105 °C. For biomass and semi-coke, Stage B

consisted of the release of volatiles and combustion, and Stage C1 was combustion of the biomass char. Stage C2 represented the combustion of semi-coke volatiles, and Stage D was the combustion of fixed carbon and minerals decomposition [4]. For the blends, Stage B consisted mainly of the burning of volatiles in the biomass. Stage C was mostly the combustion of char in the biomass and of the volatiles in the semi-coke. Similarly, Stage D was the fixed carbon combustion and minerals decomposition in the semi-coke.

Table 2 shows the temperature ranges of three different weight loss regions, the weight loss in each of these stages and the final residue of samples after combustion. The initial temperature in Stage B and the final temperature in Stage D were taken as the respective temperatures of combustion [17]. The devolatization of semi-coke begins at a higher temperature than that of biomass: at 305 °C and 190 °C, respectively. For all the blends, Stages B, C and D proceed in the same temperature ranges, which suggests that the former reveal similar combustion behaviour. In Stage D, the weight loss of blends was very similar, which is indicative that different kinds of biomass had not affected the fixed carbon combustion and minerals decomposition in the semi-coke. From Table 2 it can be seen that the residual weight of each sample was higher than their ash content (as seen in the A_{ad} values for each sample in Table 1). So, the whole combustion conversion was not 100%.

Figures 3–8 show the variation of DTG curves with temperature in different oxygen–nitrogen mixtures at a constant heating rate of 20 °C/min. The experimental curve of biomass mixed with semi-coke showed the same stages. Table 3 shows that the maximum and average weight loss rates increased with increasing oxygen concentration, and the maximum temperature (T_{max}) shifted to a lower level. The average rate of combustion of rice husks was much lower than that of three other kinds of biomass, suggesting that the ash content of the former is much higher than that of the latter. In contrast, the maximum weight loss rate in Stage D declined as the oxygen concentration increased, indicating that the fixed carbon combustion and minerals decomposition in semi-coke could be inhibited.

Table 2. Temperature intervals, weight losses and residues of samples

Sample	Temperature interval, °C			Weight loss, %			Residue, %
	Stage B	Stage C	Stage D	Stage B	Stage C	Stage D	
CS	194-380	380-551	–	59.2	26.1	–	7.05
SW	190-379	379-585	–	52.9	26.6	–	14.01
RH	191-384	384-587	–	38.8	21.5	–	35.38
SD	193-391	391-593	–	62.6	24.4	–	8.14
SC	–	305-639	639-680	–	13.1	1.7	83.52
CSSC	194-376	376-629	629-680	13.4	15.5	1.5	67.12
SWSC	190-375	375-629	629-680	11.3	15.4	1.5	69.58
RHSC	191-377	377-630	630-680	9.0	15.1	1.5	72.99
SDSC	193-391	391-635	635-710	13.2	15.4	1.5	68.02

DTG curves at different oxygen concentrations

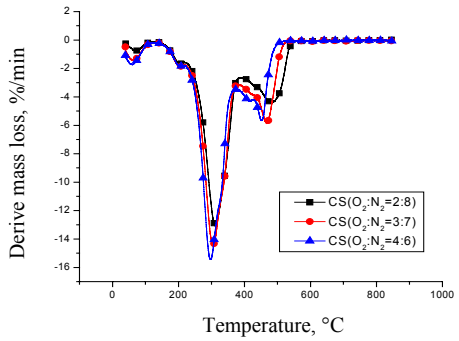

Fig. 3. DTG profiles of CS at different oxygen concentrations.

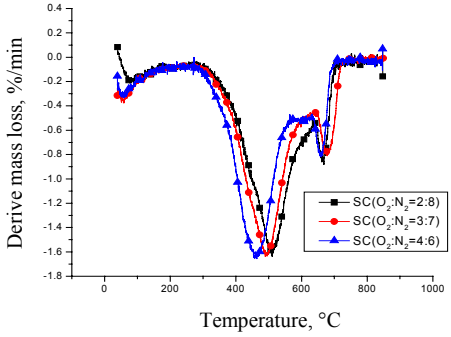

Fig. 4. DTG profiles of SC at different oxygen concentrations

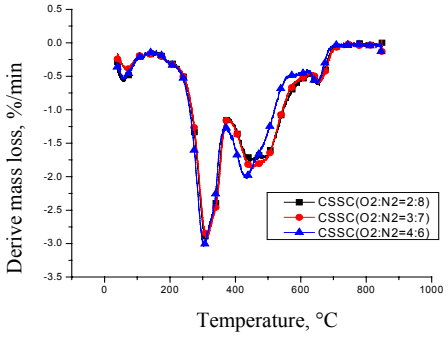

Fig. 5. DTG profiles of CSSC at different oxygen concentrations.

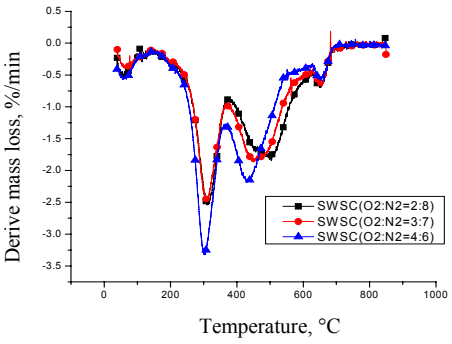

Fig. 6. DTG profiles of SWSC at different oxygen concentrations.

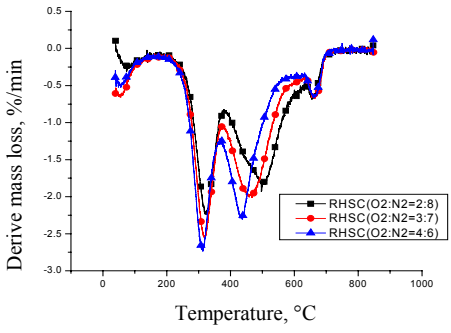

Fig. 7. DTG profiles of RHSC at different oxygen concentrations.

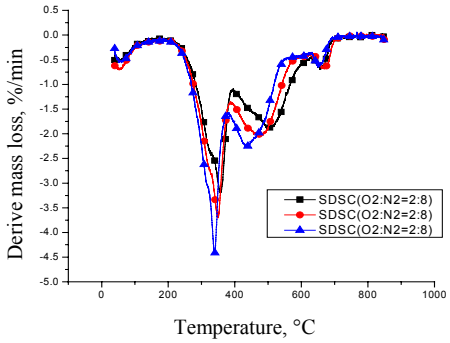

Fig. 8. DTG profiles of SDSC at different oxygen concentrations.

Table 3. **The combustion characteristics of samples at different oxygen concentrations**

Sample	N_2:O_2	T_i, °C	T_h, °C	Peak temperature, T_{max}			$(dW/dt)^c_{max}$, %/s			$(dW/dt)^c_{mean}$, %/s	S $\times 10^{-7}$
				B	C	D	B	C	D		
CS	8:2	265.43	531.36	309.20	478.97	–	13.12	4.41	–	0.0796	147
	7:3	259.71	519.35	306.18	467.73	–	14.43	5.90	–	0.0841	178
	6:4	257.7	497.04	296.46	451.62	–	15.46	5.72	–	0.0885	204
SW	8:2	256.65	544.60	312.70	492.20	–	11.62	3.70	–	0.0671	117
RH	8:2	275.83	547.44	321.82	496.94	–	9.51	2.96	–	0.0507	62.9
SD	8:2	293.51	557.86	356.95	512.91	–	14.97	3.75	–	0.0750	129
SC	8:2	419.23	695.24	–	509.20	667.62	–	1.61	0.84	0.0123	1.11
	7:3	405.24	693.54	–	494.43	668.52	–	1.62	0.81	0.0123	1.21
	6:4	380.1	689.03	–	460.59	657.93	–	1.65	0.81	0.0130	1.47
	8:2	267.26	683.15	310.29	456.14	651.61	2.92	1.75	0.61	0.0206	8.35
CSSC	7:3	264.83	676.61	312.49	443.50	653.62	2.91	1.86	0.61	0.0210	8.63
	6:4	262.69	668.92	302.03	431.39	650.93	3.02	2.02	0.60	0.0225	9.75
SWSC	8:2	262.31	683.57	309.67	499.23	649.24	2.54	1.79	0.69	0.0190	6.94
	7:3	260.34	676.48	307.02	448.98	649.01	2.46	1.84	0.65	0.0201	7.20
	6:4	259.33	669.04	302.44	430.47	650.07	3.31	2.18	0.57	0.0211	10.2
RHSC	8:2	279.28	680.31	323.17	497.14	655.10	2.23	1.93	0.68	0.0173	4.91
	7:3	276.38	674.98	318.34	458.70	664.19	2.55	1.99	0.67	0.0185	6.11
	6:4	272.01	672.89	312.69	432.80	664.05	2.72	2.28	0.65	0.0188	6.86
SDSC	8:2	297.73	681.89	357.12	501.21	658.37	3.19	1.88	0.68	0.0203	7.28
	7:3	295.92	676.27	348.39	480.84	669.35	3.70	2.03	0.67	0.0217	9.09
	6:4	293.58	666.63	335.98	434.32	651.28	4.42	2.25	0.61	0.0226	11.4

The ignition and burnout temperatures are also used to describe the combustion behavior of fuels. The ignition temperature, T_i, was determined using the TG-DTG extrapolation method [18]. The burnout temperature, T_h, was defined as the temperature at which the weight of a sample remains unchanged. It was found that the lower the ignition temperature the easier the ignition of the fuel. The lower the burnout temperature, the shorter the burnout time of the fuel, and the lower the combustible matter content of the ash. It is obvious that the initial ignition and burnout temperatures of samples decreased gradually with increasing oxygen concentration, which indicated that the ignition and burnout performances of samples could be improved.

Others have proposed that the combustion performance index, S, [19] be used to evaluate the pattern of combustion. S is computed as follows:

$$S = \frac{(dW/dt)^c_{\max} \times (dW/dt)^c_{mean}}{T_i^2 \times T_h}, \tag{1}$$

where, $(dW/dt)^c_{max}$ – maximum average weight loss rate,
$(dW/dt)^c_{mean}$ – average weight loss rate,
T_i – ignition temperature, and
T_h – burnout temperature.

The result is that the higher the value of *S*, the higher the combustion activity of the sample. The values of *S* at different oxygen concentrations are shown in Table 3 from which it is clear that the *S* values increase with increasing oxygen concentration.

Analysis of interaction

In order to understand if there is any interaction between oil shale semi-coke and biomass, the theoretical DTG curves were calculated using Eq. (2), below. The calculations are based on the experimental data from combustion of oil shale semi-coke, corn stalks and straw gathered at the same temperature. The theoretical curves represent the sum of the curves for individual components in the blends:

$$(dW/dt)_{cal} = x_1(dW/dt)_1 + x_2(dW/dt)_2\,, \tag{2}$$

where, x_1 – mass fraction of oil shale semi-coke in the blend,
x_2 – mass fraction of biomass in the blend,
$(\mathrm{d}W/\mathrm{d}t)_1$ – weight loss rate for the semi-coke (%/min), and
$(\mathrm{d}W/\mathrm{d}t)_2$ – weight loss rate of biomass (%/min).

The experimental and calculated DTG curves of samples CSSC and SWSC at a heating rate of 20 °C/min are given in Fig. 9. It can be seen that an interaction existed in the co-combustion stage. The experimental DTG curves move to a region of lower temperatures and the maximum burning rates increase in the temperature range from 190 °C to 380 °C. The reason is that semi-coke released some volatiles so that the combustion of biomass was promoted slightly. At the same time, in the temperature range of from 380 °C to 630 °C the experimental DTG curves deviate significantly from the calculated, which can be accounted for by the combustion of fixed carbon in the biomass. It is obvious that the burnout temperature of the experimental DTG curves decreased, which indicates that biomass improved the burnout performance of blends.

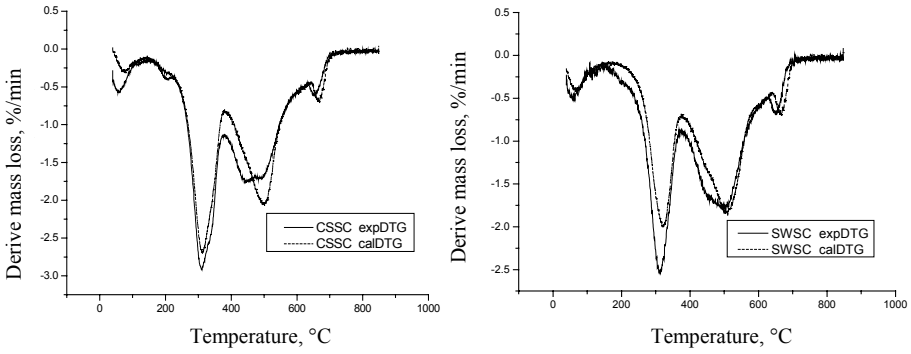

Fig. 9. Experimental DTG curves and DTG curves calculated using Eq. (2) at a heating rate of 20 °C/min for blends of CSSC and CWSC.

Kinetic analysis

The influence of temperature on combustion can be described by the Arrhenius Equation and power law approach, as follows:

$$d\alpha / dt = kf(\alpha), \tag{3}$$

$$k = A\exp(-E/RT), \tag{4}$$

where, $f(\alpha)$ = a hypothetical model of the reaction mechanism,
k – reaction rate,
A – pre-exponential factor (min^{-1}),
E – activation energy (kJ mol^{-1}),
R – ideal gas law constant (8.314 J $K^{-1}mol^{-1}$),
T – absolute temperature (K),
t – time (min), and
α – mass conversion ratio.

This can be calculated by the following relationship:

$$\alpha = (m_0 - m_t)/(m_0 - m_f), \tag{5}$$

where, m_0 – initial mass of the sample,
m_t – mass of the sample at time t, and
m_f – final mass of the sample.

For a constant heating rate β (K min^{-1}) during combustion $\beta = dT/dt$, Eqs. (3 & 4) can be combined into:

$$\frac{d\alpha}{f(\alpha)} = \frac{A}{\beta}\exp\left(-\frac{E}{RT}\right)dT. \tag{6}$$

Integrating Eq. (6) gives:

$$G(\alpha) = \int_0^{\alpha} d\alpha / f(\alpha) = A/\beta \int_{T_0}^{T} \exp(-E/RT)dT, \tag{7}$$

where, $G(\alpha)$ is the integral function of conversion.

Eq. (6) is integrated by using the Coats–Redfern Method [20], yielding:

$$\ln\left[\frac{G(\alpha)}{T^2}\right] = \ln\left[\frac{AR}{\beta E}\left(1 - \frac{2RT}{E}\right)\right] - \frac{E}{RT}. \tag{8}$$

The function $G(\alpha)$ depends on the controlling mechanism of the reaction and the size and shape of the reacting particles [19]. Table 4 shows the expressions of $G(\alpha)$ for the basic model functions usually used to study the kinetics of solid-state reactions. Using these functions, it was possible to estimate the reaction mechanisms governing the process of combustion. The form of $G(\alpha)$, which gives the highest correlation coefficient, will be considered as the best function for the model.

The kinetics models of O1, O2 and O3 are the first-order, second-order and third-order chemical reactions, respectively. R2 is used for a circular disc reacting from the edge inward, while R3 is used for a sphere which reacts from the surface inward. This mechanism is assumed to be the governing conversion model in the combustion of some carbonaceous materials [21]. In a diffusion-controlled reaction, D1 is used for a one-dimensional diffusion process governed by a parabolic law, with a constant diffusion coefficient. D2 is the function for a two-dimensional diffusion-controlled process in a cylinder. D3 is Jander's. Equation for diffusion-controlled solid-state reaction kinetics in a sphere where diffusion in all three directions is highly important. D4 is Ginstling–Brounshtein's Equation for a diffusion-controlled reaction starting from the outside of a spherical particle [22].

Table 4. **Expressions of $G(\alpha)$ for kinetic model functions employed for solid-state reactions**

Mechanism	Model	$G(\alpha)$
Reaction order	O1	$-\ln(1-\alpha)$
	O2	$(1-\alpha)^{-1}$
	O3	$(1-\alpha)^{-2}$
Phase boundary controlled reaction	R2	$1-(1-\alpha)^{1/2}$
	R3	$1-(1-\alpha)^{1/3}$
Diffusion	D1	α^2
	D2	$(1-\alpha)\ln(1-\alpha)+\alpha$
	D3	$[1-(1-\alpha)^{1/3}]^2$
	D4	$1-2\alpha/3-(1-\alpha)^{2/3}$

In Stage B of corn straw combustion, models R2, R3, D1, D2, D3 and D4 had higher values of correlation coefficients, i.e. between 0.9800 and 0.9900 (data not shown). However, Model O1 showed the highest values of correlation coefficients for all the samples, exceeding 0.9900 (Table 5). In Stage C1 of corn stalk combustion, Models D3 and D4 had the highest values of correlation coefficients, higher than 0.9900. The results of Model D4 are given in Table 5, while the other models exhibited correlation coefficient values between 0.9500 and 0.9900. In Stage C2 of semi-coke combustion, Model O1 had the highest values of correlation coefficients, around 0.9900. For Stage D, Model D4 had the highest correlation coefficient values. Model O1 displayed the highest values of correlation coefficients for Stage B of all blends (data not shown). For Stage C of blends combustion, Models O1, D3, D4 displayed the highest values of correlation coefficients, around 0.9900. Thus, the results confirm that Model O1 is the

most representative solid-state mechanism for Stage C of blends combustion. Model D4 was found to be the best-fit for Stage D of blends combustion.

Table 5. **The activation energy of oxidative pyrolysis**

Sample	N_2:O_2	Stage B		Stage C		Stage D	
		E	R^2	E	R^2	E	R^2
CS	8:2	54.45	0.9929	25.28	0.9930	—	—
	7:3	52.05	0.9967	28.03	0.9989	—	—
	6:4	52.78	0.9951	25.73	0.9905	—	—
SC	8:2	—	—	47.96	0.9949	60.29	0.9948
	7:3	—	—	39.90	0.9929	56.69	0.9964
	6:4	—	—	38.85	0.9925	57.58	0.9926
CSSC	8:2	38.85	0.9974	19.57	0.9912	16.33	0.9969
	7:3	41.41	0.9886	20.92	0.9928	16.85	0.9956
	6:4	40.82	0.9890	19.79	0.9913	16.29	0.9973
SWSC	8:2	34.02	0.9899	21.95	0.9903	18.75	0.9956
	7:3	38.26	0.9973	22.06	0.9951	22.31	0.9918
	6:4	38.50	0.9984	19.73	0.9999	18.05	0.9899
RHSC	8:2	44.68	0.9976	25.49	0.9947	27.81	0.9976
	7:3	39.37	0.9968	23.53	0.9967	21.00	0.9996
	6:4	45.61	0.9980	22.68	0.9937	28.61	0.9905
SDSC	8:2	44.66	0.9968	22.12	0.9957	23.12	0.9905
	7:3	42.62	0.9970	21.23	0.9941	21.58	0.9963
	6:4	50.29	0.9945	21.74	0.9957	19.64	0.9941

Conclusions

Biomass samples experienced two-stage combustion. In the first stage the combustion of the volatile occurred from 190 °C to 360 °C. In the second stage the combustion of fixed carbon took place between 380 °C and 590 °C. Oil shale semi-coke also underwent combustion in two stages: *viz*. between 305 °C and 639 °C, at which volatiles were released and burned, and between 639 °C and 680 °C, at which the char combustion and minerals decomposition occurred. However, semi-coke/biomass blends underwent three combustion steps.

The maximum values of DTG curves shifted to lower temperatures with increasing oxygen concentration. This shows that oxygen enrichment can shorten burning time and improve combustion activity. Peak, ignition and burnout temperatures all decrease with increases in oxygen concentration. The higher oxygen concentration clearly results in higher weight loss rates.

The co-combustion of oil shale semi-coke and biomass is a complicated multistage process, during which interaction between components occurs. Biomass improves the combustion performance of blends.

The results of the kinetic analysis show that the O1 mechanism is the one mainly responsible for Stage B of biomass combustion, Stage C2 of semi-

coke combustion, as well as stages B and C of blends combustion. On the other hand, D3 and D4 diffusion mechanisms are governing Stage C1 of the biomass combustion, while the D4 diffusion mechanism is responsible for Stage D of semi-coke and blends combustion.

Acknowledgments

The authors are grateful for financial support from the Department of Education of Jilin Province (2009106).

REFERENCES

1. *Qian, J. L., Yi, L., Wang, J .Q.* Oil Shale-Oil Supplements Energy. – Beijing: China Petrochemical Press, 2008 [in Chinese].
2. *Wang, Q., Xu, F., Bai, J. R.* Study on basic physical and chemical characteristics of Huadian oil shale // Journal of Jilin University (Earth Science Edition). 2006. Vol. 36, No. 6. P. 720–724.
3. *Wang, Q., Wu, X. H., Sun, B. Z.* Combustion reaction kinetics study of Huadian oil shale semi-coke // Proceedings of the CSEE. 2006. Vol. 26. No. 7. P. 29–34 [in Chinese].
4. *Wang, Q., Sun, B. Z., Wu, X. H.* Influence of retorting temperature on combustion characteristics and kinetic parameters of oil shale semicoke // Oil Shale. 2006. Vol. 23, No. 4. P. 328–339.
5. *Wang, Q., Sun, B. Z., Wu, X. H.* Study on combustion characteristics of mixtures of Huadian oil shale and semicoke // Oil Shale. 2007. Vol. 24, No. 2. P. 135–145.
6. *Wang, Q., Wang, H. G., Sun, B. Z.* Interactions between oil shale and its semicoke during co-combustion // Fuel. 2009. Vol. 88, No. 8. P. 1520–1529.
7. *Trikkel, A., Kuusik, R., Martins, A., Pihu, T., Stencel, J. M.* Utilization of Estonian oil shale semicoke // Fuel Process. Technol. 2008. Vol. 89, No. 8. P. 756–763.
8. *Arro, H., Prikk, A., Pihu, A., Opik, I.* Utilization of semi-coke of Estonian shale oil industry // Oil Shale. 2002. Vol. 19, No. 2. P. 117–125.
9. *Dai, J., Grace, J. R.* Biomass screw feeding with tapered and extended sections // Powder Technol. 2008. Vol. 186, No. 1. P. 56–64.
10. *Gil, M. V., Casal, D., Pevida, C., Pis, J. J., Rubiera, F.* Thermal behaviour and kinetics of coal/biomass blends during co-combustion // Bioresource Technol. 2010. Vol. 101, No. 14. P. 5601–5608.
11. *Baxter, L.* Biomass-coal co-combustion: opportunity for affordable renewable energy // Fuel. 2005. Vol. 84, No. 10. P. 1295–1302.
12. *Haykiri-Acma, H., Yaman, S.* Effect of biomass on burnouts of Turkish lignites during co-firing // Energ. Convers. Manage. 2009. Vol. 50, No. 9. P. 2422–2427.
13. *Liu, N. A., Fan, W. C., Dobashi, R., Huang, L. S.* Kinetic modeling of thermal decomposition of natural cellulosic materials in air atmosphere // J. Anal. Appl. Pyrol. 2002. Vol. 63, No. 2. P. 303–325.

14. *Fang, M. X., Shen, D. K., Li, Y. X., Yu, C. J., Luo, Z. Y., Cen, K. F.* Kinetic study on pyrolysis and combustion of wood under different oxygen concentrations by using TG-FTIR analysis // J. Anal. Appl. Pyrol. 2006. Vol. 77, No. 1. P. 22–27.
15. *Yu, Z. S., Ma, X. Q., Liu, A.* Thermogravimetric analysis of rice and wheat straw catalytic combustion in air-and oxygen-enriched atmospheres // Energ. Convers. Manage. 2009. Vol. 50, No. 3. P. 561–566.
16. *Luo, S. Y., Xiao, B., Hu, Z. Q., Liu S. M., Guan, Y. W.* Experimental study on oxygen-enriched combustion of biomass micro fuel // Energy. 2009. Vol. 34, No. 11. P. 1880–1884.
17. *Rubiera, F., Arenillas, A., Fuente, E., Miles, N., Pis, J. J.* Effect of the grinding behaviour of coal blends on coal utilisation for combustion // Powder Technol. 1999. Vol. 105, No. 1–3. P. 351–356.
18. *Yu Qiumei, Pang Yajun, Chen Hongguo.* Determination of ignition points in coal-combustion tests // North China Electric Power (China). 2001. Vol. 7. P. 9–10 [in Chinese].
19. *Nie, Q. H., Sun, S. Z., Li, Z. Q.* Thermogravimetric analysis on the combustion characteristics of brown coal blends // Combust. Sci. Technol. 2001. Vol. 7, No. 1. P. 71–76.
20. *Hu, R. Z., Gao, S. L., Zhao, F. Q.* Thermal Analysis Kinetics. – Beijing: Science Press, 2007 [in Chinese].
21. *López-Fonseca, R., Landa, I., Elizundia, U., Gutiérrez-Ortiz, M. A., González-Velasco, J. R.* Thermokinetic modeling of the combustion of carbonaceous particulate matter // Combust. Flame. 2006. Vol. 144. No. 1-2. P. 398–406.
22. *Alshehri, S. M., Monshi, M. A. S., Abd El-Salam, N. M., Mahfouz, R. M.* Kinetics of the thermal decomposition of γ-irradiated cobaltous acetate // Thermochimica Acta. 2000. Vol. 363, No. 1–2. P. 61–70.

Presented by V. Oja
Received October 3, 2010